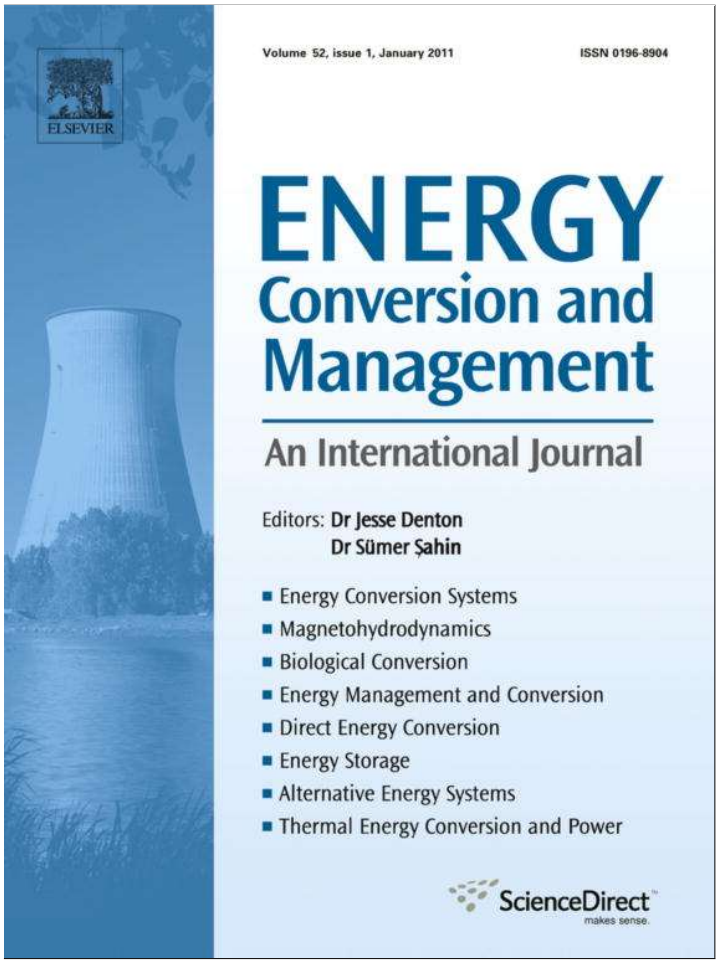

Energy Conversion and Management 52 (2011) 391–396

Contents lists available at ScienceDirect

Energy Conversion and Management

journal homepage: www.elsevier.com/locate/enconman

Analytic synthesis of a hysteresis motor

Linus U. Anih, Emeka S. Obe *, Eugene O. Agbachi

Department of Electrical Engineering, University of Nigeria, Nsukka, Nigeria

ARTICLE INFO

Article history:
Received 20 November 2009
Accepted 8 July 2010
Available online 2 August 2010

Keywords:
High rotor resistance to leakage reactance r_2/x_2 ratio
Inverted torque–speed characteristics
Mechanically coupled machines
Transfer field (TF) machine

ABSTRACT

This paper presents the unique synthesis of a motor with a hysteresis torque–speed characteristic. The machine is synthesized from a conventional polyphase squirrel cage induction motor (SCIM) with a high rotor resistance to leakage reactance r_2/x_2 ratio, which is mechanically coupled to a polyphase transfer field (TF) machine but with an inversion of the usual torque–speed characteristic of the latter about the speed axis and both machines are connected in parallel to the supply. It is shown that the resultant torque of the combined machines is constant, from standstill to full speed ω_0, typical of that of a hysteresis motor. Unlike the conventional hysteresis motor, the output torque of the synthesized version can be made large.

1. Introduction

The induction motor is the most common of all ac motors and has been variously described as the "work-horse" of industry. In its normal working range, the speed of the induction motor remains reasonably constant, varying only slightly with load. For this reason, it is regarded for all intents and purposes as a constant speed motor. The major shortcoming of the induction motor is the relative low power factor which is always lagging.

Synchronous machines on the other hand are constant speed machines with controllable power factor, which can be made leading. However, they are more expensive to produce due to slip rings and brushes compared to squirrel cage induction motors. The major demerit of synchronous machines is the problem of synchronization. The polyphase reluctance motor on the other hand operates at a fixed speed, synchronous speed of the rotating magnetic field. The major differences between the reluctance and synchronous machines are the absence of rotating windings and dc excitation in the rotors of reluctance machines. The major disadvantage of the reluctance machine apart from the relatively low power factor due to excessive reactive magnetizing current is the synchronizing problems. The pull-in torque is generally less than half of the pull-out torque. A reluctance motor is therefore several times larger than a synchronous motor with dc excitation having the same horse power and speed ratings. However, in some applications these disadvantages may be off set by its simplicity of construction, no slip rings, no brushes and no dc field winding, low cost and practically maintenance free operation.

The hysteresis motor, like the reluctance motor does not have a dc excitation and rotor windings. Unlike the reluctance motor, however, the hysteresis motor does not have a salient rotor. The rotor of a hysteresis motor has a ring of special magnetic material, such as chrome hard steel or cobalt, mounted on a cylinder of aluminum or some other non-magnetic material having high retentivity, so that the hysteresis loss is high. The rotor of the ideal machine is assumed to have zero conductivity and so no torque is produced as a result of induced currents in the rotor circuit. The motor torque therefore would be entirely due to hysteresis effects.

The stator field and the induced rotor field are present at all speeds from zero up to synchronous speed where the rotor is no longer subject to alternating magnetization. The torque is constant throughout and the motor is therefore self-starting. The hysteresis motor is the smoothest and the quietest running ac machine because of the smooth rotor periphery and freedom from mechanical and magnetic vibrations. These characteristics have endeared it to such applications as in quality sound reproduction equipment, record player motors, electric clocks and other timing devices. In contrast with a reluctance motor, which must "snap" its load into synchronism from an induction motor torque–speed characteristic, a hysteresis motor can synchronize any load which it can accelerate, no matter how great the inertia and no other electrical machine possesses this unique feature. The major limitation of the hysteresis motor is its specific low output power which has narrowed its applications to low power devices. The output power is about one-quarter of an induction motor of the same dimensions. Hysteresis motors are generally available as fractional horse power

* Corresponding author. Tel.: +234 803 053 7642.
E-mail addresses: luanih@yahoo.com (L.U. Anih), obeunn@yahoo.com (E.S. Obe), okennagbachi@yahoo.com (E.O. Agbachi).

0196-8904/$ - see front matter © 2010 Elsevier Ltd. All rights reserved.
doi:10.1016/j.enconman.2010.07.014

motors and most of the studies on the machine were skewed towards production of the machine by exploiting hysteresis loss phenomena of magnetic materials [1–3]. In this paper, an entirely different approach is adopted towards producing a hysteresis motor with good output power by synthesis from ac machines with well known output power characteristics. Agu [4] has suggested that the synthesis of a hysteresis motor from two induction motors could be possible if one of the motors could be made to operate with inverted torque–speed characteristics. This paper is an extension of the work done in Ref. [4] and presents a simple method of deriving negative torque in the low-speed region $0 \leqslant \omega < \omega_0/2$ and positive torque in the high speed region $\omega_0/2 < \omega \leqslant \omega_0$ from a transfer field (TF) machine so that the combination of its torque–speed characteristic with that of a squirrel cage induction motor (SCIM) with high rotor resistance to leakage reactance ratio will result in a hysteresis motor torque–speed characteristic.

2. Transfer field (TF) machine

The stable operation of a polyphase induction motor at one-half normal speed by means of unbalanced impedance in the rotor circuit is well known as Gorges phenomenon [5]. The half-speed operation did not receive industrial acceptance because of the associated vibration and noise due to injection of low frequency current of $(\omega_0 - 2\omega)$ into the supply system. Broadway and Tan [6] improved the industrial acceptance by mechanically coupling two identical machine elements together and connecting their windings in parallel to the supply and thus creating a local loop between the machine windings for the circulation of the low frequency currents of $(\omega_0 - 2\omega)$ and thus diverted from the supply. Agu [7] evolved a configuration of a composite two-element reluctance effect machine known as the transfer field (TF) machine. Unlike [6], there are no windings in the rotor, including damper windings. Instead, there are two windings on each unit stator comprising the TF machine, known as the main and auxiliary windings. The main windings are connected in series while the auxiliary windings are transposed (anti-series) in passing from one unit machine to the other. Like [6], the rotors of the two machine elements are salient in configuration and in space quadrature as shown in Fig. 1. Cathey and Nasar [8] studied the steady-state equivalent circuit of the TF machine for asynchronous operation while Anih and Obe [9] studied the dynamic performance of the TF machine.

In the TF machine arrangement, the low frequency current of $(\omega_0 - 2\omega)$ is confined to circulate in the auxiliary windings and thus prevented from interfering with the supply [7]. Furthermore, there is a complete electrical separation of the winding carrying the mains supply current of ω_0 frequency from that which carries the low frequency current of $(\omega_0 - 2\omega)$. However, the two windings are magnetically coupled. Additionally, the auxiliary winding terminals are accessible for control purposes. An alternative configuration of the TF machine can be obtained by holding one-half of the machine stator and rotor while the other half stator and rotor is rotated until the pole-axis of the two halves are in alignment; and the axes of the main windings are out of phase by 90° electrical degrees and the alignment of the axes of the auxiliary windings in reduced from 180° to 90° electrical degrees [10].

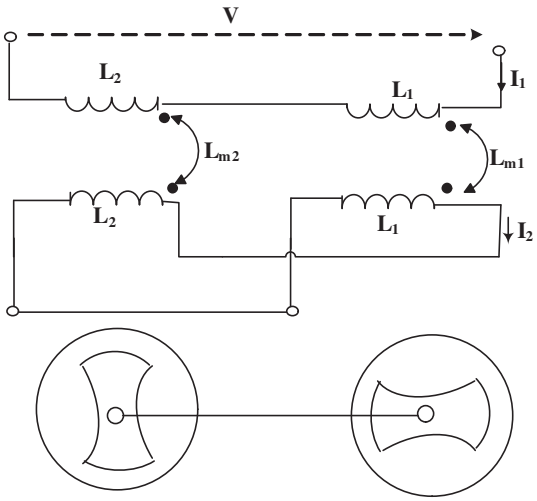

Fig. 1. Per-phase coupled coil representation of the TF machine.

2.1. Principle of operation of the TF machine

The main winding is connected to the source and draws a current I_0 at frequency ω_0 which produces an mmf whose distribution is expressed as

$$m_0 = M_0 \cos(\theta - \omega_0 t) \tag{1}$$

The air–gap permeance distribution in the two halves of the machine may be expressed respectively as

$$P_A = P_0 + P_V \cos 2(\theta - \omega t) \tag{2}$$

and

$$P_B = P_0 + P_V \cos 2\left(\theta - \omega t - \frac{\pi}{2}\right) = P_0 - P_V \cos 2(\theta - \omega t) \tag{3}$$

where ω is the rotor speed.

The corresponding flux distribution in the air–gap of the respective halves of the TF machine due to the mmf m_0 is obtained from the product of Eq. (1) and Eq. (2) or Eq. (3). If space harmonics are neglected, the flux distribution are given by

$$\begin{aligned} B_A &= M_0 P_0 \cos(\theta - \omega_0 t) + \frac{M_0 P_V}{2} \cos(\theta + (\omega_0 - 2\omega)t) \\ &= B_{01} \cos(\theta - \omega_0 t) + B_{02} \cos(\theta + (\omega_0 - 2\omega)t) \end{aligned} \tag{4}$$

and

$$\begin{aligned} B_B &= M_0 P_0 \cos(\theta - \omega_0 t) - \frac{M_0 P_V}{2} \cos(\theta + (\omega_0 - 2\omega)t) \\ &= B_{01} \cos(\theta - \omega_0 t) - B_{02} \cos(\theta + (\omega_0 - 2\omega)t) \end{aligned} \tag{5}$$

From Eqs. (4) and (5) above, the average net flux linking the main windings is obtained by their summation and is given by

$$B_m = B_{01} \cos(\theta - \omega_0 t) \tag{6}$$

This flux rotates in the positive anti-clockwise direction and is behind the magnetizing reactance of the winding. The distribution of the average flux linking the auxiliary winding is obtained by the subtraction of Eq. (5) from Eq. (4) and is given by

$$B_a = B_{02} \cos(\theta + (\omega_0 - 2\omega)t) \tag{7}$$

This flux rotates in the negative clockwise direction for $\omega < 1/2\omega_0$ and will induce emfs of $(\omega_0 - 2\omega)$ frequency in the auxiliary windings which will circulate current I_2 in the short-circuited winding, which is inversely proportional to its leakage impedance. The emfs induced in the auxiliary windings are additive because of the transposition of the auxiliary windings.

For an emf E_2 induced in the auxiliary winding, the current circulating in the winding is given by

$$I_2 = \frac{2E_2 \cos((\omega_0 - 2\omega)t - \varphi)}{\sqrt{r_e^2 + (\omega_0 - 2\omega)^2 l_e^2}} \tag{8}$$

where φ is the impedance angle, r_e and l_e are the effective resistance and inductance of the auxiliary winding respectively.

The circulation of current in the auxiliary winding will cause the main winding to draw an additional current I_1 from the source which will balance the auxiliary winding current reflected in the main winding, in a manner similar to what is obtained in a transformer and induction motors. An equilibrium condition is attained when the emf induced in the auxiliary winding by the flux due to I_1 balances the self-induced emf due to I_2 in the auxiliary windings. The torque of the machine is due to the interaction between the main and auxiliary winding mmfs in the respective halves of the machine. If the auxiliary winding mmf supports the main winding mmf in one-half of the TF machine say, it will oppose it in the other half due to the transposition of the auxiliary winding. When the torque is maximum in one-half, it is zero in the other half and the load torque swings cyclically from one machine half to the other while the net torque remains constant. The roles of the main and auxiliary windings can be interchanged and will produce the same result.

2.2. Torque–speed characteristic of the TF machine

When the auxiliary winding is on open circuit, the machine does not develop torque because there are no rotor windings which would produce an induction motor type torque. Furthermore, since the self impedance of the machine windings does not change with rotor angular position, there would be no reluctance torque either. However, when the auxiliary winding is closed, the emf E_2 induced in the auxiliary winding, will circulate current I_2 in the winding. The voltage induced in the auxiliary winding is directly proportional to $(\omega_0 - 2\omega)$ as can be deduced from Eq. (7). When the rotor moves at the speed $\omega = 1/2\omega_0$, the emf induced in the auxiliary winding is zero and so is the auxiliary winding current I_2. Consequently, the torque of the machine is zero at $\omega = 1/2\omega_0$.

The cyclic variation of the mutual coupling between the main and auxiliary windings with rotor angular position is the basis of electromagnetic torque development of the machine. An analogous relationship exists between the stator and rotor windings of an induction motor. The asynchronous torque–speed characteristic as should be expected resembles that of conventional induction motor operating at half the synchronous speed as shown in Fig. 2 [7–9,11], curve '*A*'. The torque can be readily derived [9] as:

$$T = \frac{6I_2'^2 r_2'}{\omega_0(2s-1)} \tag{9}$$

where s is the slip, r_2' is the auxiliary winding resistance referred to the main winding and I_2' is the auxiliary winding current referred to the main winding.

In the speed range, $0 \leqslant \omega \leqslant 1/2\omega_0$ the machine is motoring and in the range $1/2\omega_0 \leqslant \omega \leqslant \omega_0$, the machine is generating as depicted by curve '*A*'. When motoring, the axis of the resultant air gap mmf in each half of the TF machine would lead the axis of the rotor pole and would lag behind it for the generating mode [11].

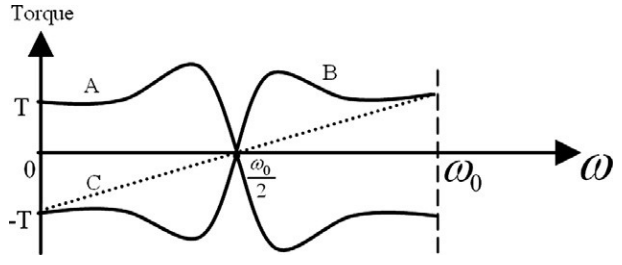

Fig. 2. The torque–speed characteristics of the TF machine showing the effect of the leading pf and high (r_2/x_2) ratio.

3. Review of current loci of asynchronous motors

The rotor circuit voltage equation of an induction motor in phasor form can be written from its equivalent circuit of Fig. 3 as:

$$E_2 = I_2\left(\frac{r_2}{s} + jx_2\right) \tag{10}$$

From (10), the per-phase rotor current at any slip s is given by:

$$I_2 = \frac{E_2}{\sqrt{\left(\frac{r_2}{s}\right)^2 + x_2^2}\angle \arctan(\varphi_2)} \tag{11}$$

where

$$\varphi_2 = \frac{sx_2}{r_2} \tag{12}$$

and the rotor current lags the rotor voltage E_2 by φ_2

The power input to the rotor is given by:

$$P_g = E_2 I_2 \cos\varphi_2 \tag{13}$$

The power factor $\cos\varphi_2$ may be expressed as:

$$\cos\varphi_2 = \frac{\text{Per-phase rotor resistance}}{\text{Per-phase rotor impedance}} = \frac{r_2/s}{\sqrt{(r_2/s)^2 + x_2^2}} \tag{14}$$

Therefore, (13) becomes:

$$P_g = E_2 I_2 \frac{r_2/s}{\sqrt{(r_2/s)^2 + x_2^2}} = I_2^2 r_2/s \tag{15}$$

P_g is actually the power transferred from the stator to the rotor across the air–gap. For the purpose of obtaining the rotor current locus, (10) can be rewritten as:

$$\frac{-jE_2}{x_2} = I_2 - jI_2\frac{r_2}{sx_2} \tag{16a}$$

Eq. (16a) shows that a constant current E_2/x_2 lagging 90° behind E_2 is made up of two components: the current in the rotor circuit I_2 plus a variable component $I_2\frac{r_2}{sx_2}$ lagging I_2 by 90° as shown in Fig. 4.

From the geometry of the phasor diagram shown in Fig. 4, where a right-angled triangle is formed over a constant diameter E_2/x_2, it can be seen that the phasor I_2 traces out a semi-circle as $\frac{r_2}{sx_2}$ varies from 0 to ∞. If $\frac{r_2}{sx_2}$ takes negative values, implying s being traditionally negative (super synchronous speed of the rotor), Eq. (16a) modifies to:

$$\frac{-jE_2}{x_2} = I_2 + jI_2\frac{r_2}{sx_2} \tag{16b}$$

The phasor I_2 will trace out a semi-circle below the OA co-ordinate, which is the negative slip region. The phasor I_2 will now lag the applied voltage by an angle greater than 90°. This means negative power factor ($\cos\varphi_2$) or that electric power flows out of the machine from rotor to the stator resulting in generator operation $\left(P_g = -I_2^2 r_2/s\right)$, a reversal of power flow.

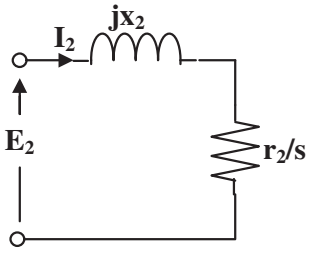

Fig. 3. Rotor equivalent circuit of an induction motor.

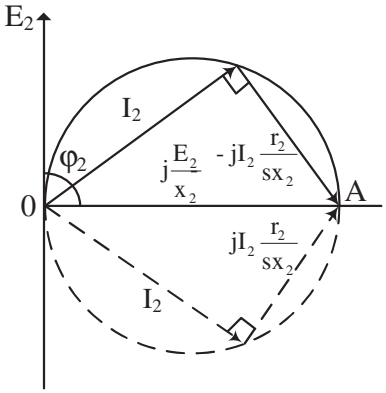

Fig. 4. Current locus for inductive rotor circuit of induction machine.

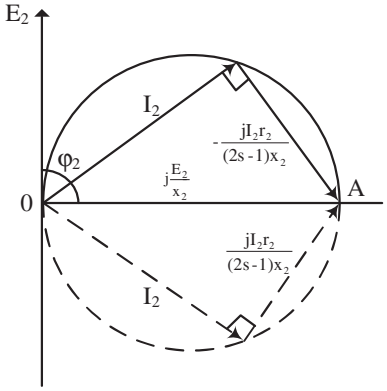

Fig. 7. Current locus of inductive auxiliary winding of a TF machine.

Suppose capacitance is injected into the rotor circuit through the slip rings and of magnitude twice that of the leakage reactance x_2 say, the overall reactance of the rotor circuit becomes $-jx_2$ even though s is positive. Eq. (16a) will now be modified to:

$$\frac{jE_2}{x_2} = I_2 + jI_2\frac{r_2}{sx_2} \tag{16c}$$

From Eq. (16c), the locus of I_2 as s varies from 0 to ∞ is as shown in Fig. 5.

It can be seen from Fig. 5 that the rotor current I_2 leads the applied voltage E_2 by $\varphi_2 > 90°$. Consequently, the leading power factor cos φ_2 is negative, which means that power flows out of the machine from the rotor to the stator resulting in generating operation $\left(P_g = -I_2^2\frac{r_2}{sx_2}\right)$. In summary, the generating operation can be obtained at rotor speeds below synchronous ($\omega < \omega_0$) by capacitive injection into the rotor circuit, such that the overall reactance of the rotor circuit becomes capacitive (i.e. injected capacitive reactance x_c is greater than the leakage reactance x_2).

Similarly, consider the auxiliary winding circuit of a transfer field (TF) machine operating in the asynchronous mode as shown in Fig. 6.

The auxiliary winding voltage equation in phasor form can be written directly from its equivalent circuit of Fig. 6 as:

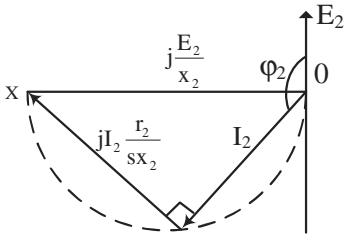

Fig. 5. Current locus for the capacitive rotor circuit of induction machine.

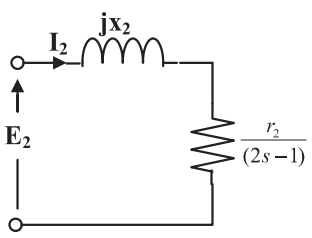

Fig. 6. Equivalent circuit of an auxiliary winding of a TF machine.

$$E_2 = I_2\left(\frac{r_2}{2s-1} + jx_2\right) \tag{17a}$$

or

$$-j\frac{E_2}{x_2} = I_2 - j\frac{I_2 r_2}{(2s-1)x_2} \tag{17b}$$

From the preceding discussion, the locus of I_2 as $\frac{r_2}{(2s-1)x_2}$ varies from 0 to ∞, that is, as s varies from 0 to 1/2 is a semi-circle above OA co-ordinate as shown in Fig. 7. If $\frac{r_2}{(2s-1)x_2}$ takes negative values, supersynchronous speed of the rotor ($\omega > 1/2\omega_0$), that is $s < 1/2$, the phasor I_2 will trace out a semi-circle below the OA co-ordinate and lags the applied voltage E_2 by an angle greater than 90°. The power factor will become negative and there will be a reversal of power flow from the auxiliary winding to the main winding, generating operation.

Alternatively, $\frac{r_2}{(2s-1)x_2}$ can be made negative by capacitive injection into the auxiliary winding while s is within the range of motor operation. Suppose a capacitance is injected into the auxiliary winding which is twice that of the leakage reactance in magnitude, the overall reactance of the auxiliary winding will become capacitive ($-x_2$). Eq. (17b) will then be modified to:

$$j\frac{E_2}{x_2} = I_2 + j\frac{I_2 r_2}{(2s-1)x_2} \tag{17c}$$

The locus of I_2 as $\frac{r_2}{(2s-1)x_2}$ varies from 0 to ∞ will be as shown in Fig. 8.

The phasor I_2 now leads the applied voltage E_2 by an angle > 90° and consequently, the power factor is negative and therefore there will be a reversal of power flow from the auxiliary winding back to the main winding. Like an induction machine, however, the main winding will still be connected to the supply for the purpose of deriving the magnetizing current.

From the discussions thus far, it follows that generating operation can be obtained from an induction machine and a TF machine without the rotor necessarily operating above the synchronous

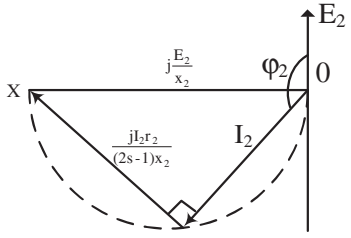

Fig. 8. Current locus of capacitive auxiliary winding of a TF machine.

speed; by injecting a capacitive reactance into the rotor and auxiliary winding respectively such that they become capacitive.

4. Effect of leading power factor

Suppose a variable capacitance is injected into the auxiliary winding of a TF machine as shown in Fig. 9 and tuned such that the overall auxiliary winding leakage reactance becomes capacitive ($jx_c > jx_1$), the current in the auxiliary winding would become reversed in phase, relative to what it is for the case of the usually inductively loaded auxiliary winding circuit, from lagging to leading.

The effect of the power factor reversal from lagging to leading will result in the shift of the axis of the resultant air–gap mmf to the trailing tips of the rotor poles in both halves of the machine, comprising the TF machine and thus leading to an electromagnetic torque in the opposite direction to the rotation of the rotor, that is, generator operation [11]. The machine would require an external mechanical agency to drive the rotor forward over the speed range $0 \leqslant \omega \leqslant 1/2\omega_0$. The torque–speed characteristic of the capacitively loaded auxiliary winding will take the form of curve '*B*' [11] as shown in Fig. 2, operating in the generating mode in the low-speed region and producing positive torque as a motor in the high speed region. If the auxiliary winding resistance to leakage reactance r_2/x_2 ratio of the winding producing curve '*B*' is made high by using conductors with small cross sectional area or by connecting resistance in series with the injected capacitance, curve '*B*' will take the form of curve '*C*'. The external prime mover requirement for generator operation is readily met by the polyphase SCIM with high rotor resistance to leakage reactance r_2/x_2 ratio which is mechanically coupled to the shaft of the TF machine.

5. The physical arrangement of the proposed hysteresis motor

The physical arrangement of the proposed hysteresis motor is shown schematically in Fig. 10. The configuration comprises a squirrel cage induction motor (SCIM) with a high rotor resistance to leakage reactance r_2/x_2 ratio which is mechanically coupled to a TF reluctance effect machine with a high auxiliary winding resistance to leakage reactance r_2/x_2 ratio as well and both connected in parallel to the supply. The two machines are wound for the same number of poles. The possibility of combining the two machines in one frame is being investigated.

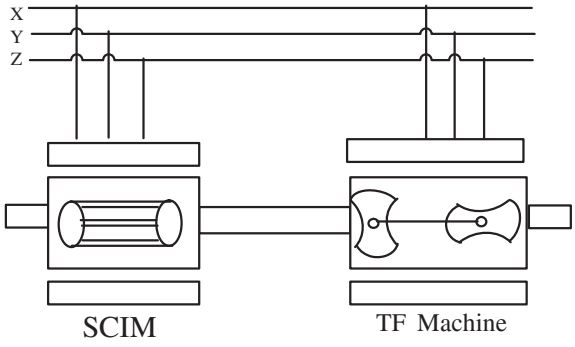

Fig. 10. Schematic arrangement of the proposed hysteresis motor.

6. Synthesis of a hysteresis motor

The torque–speed characteristic of an ideal hysteresis motor is shown in Fig. 11 as characteristic *D*.

In the speed range $0 \leqslant \omega \leqslant \omega_0$ the torque–speed characteristic can be synthesized from two linear graphs viz *A* and *B* whose equations are given respectively as:

$$T_A = 2T - \frac{2T}{\omega_0}\omega \tag{18}$$

$$T_B = -T + \frac{2T}{\omega_0}\omega \tag{19}$$

The summation of Eqs. (18) and (19) will produce graph *D*, which has a constant torque from stall to synchronous speed ω_0. Graph *A* has the shape of the torque–speed characteristic of an induction motor with a high rotor resistance to leakage reactance r_2/x_2 ratio. Graph *C* is the asynchronous torque–speed characteristic of a TF machine whose output torque is one-half of that of the SCIM with high r_2/x_2 ratio, producing Graph *A*. Graph *B* is unusual; with negative torque at starting and positive torque above the half-speed point $1/2\omega_0$ and is a mirror image of curve *C* about the horizontal axis and resembles the asynchronous torque–speed characteristic of a TF machine with capacitively loaded auxiliary winding with high r_2/x_2 ratio as discussed above.

Consider a two-pole squirrel cage induction motor say, with a high rotor resistance to leakage reactance r_2/x_2 ratio, $r_2 \approx 10x_2$, the torque–speed characteristic will produce graph *A* as shown in Fig. 12. A two-pole TF machine with a capacitively loaded auxiliary

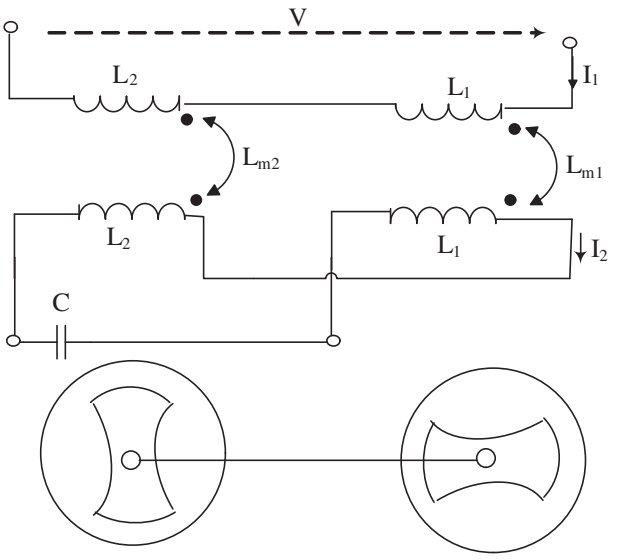

Fig. 9. Per-phase coupled coil representation of the TF machine with injected capacitance in the auxiliary winding.

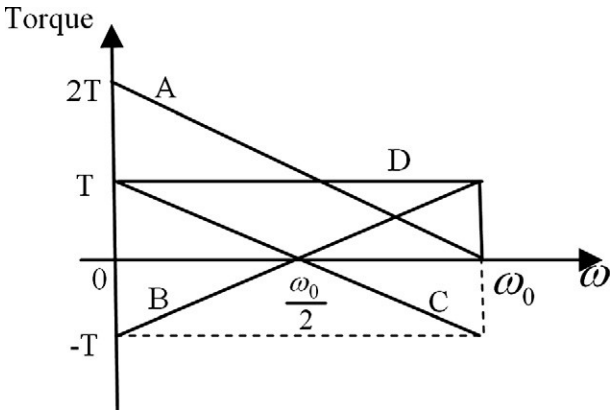

Fig. 11. The idealized torque–speed characteristics of a hysteresis motor and component torques.

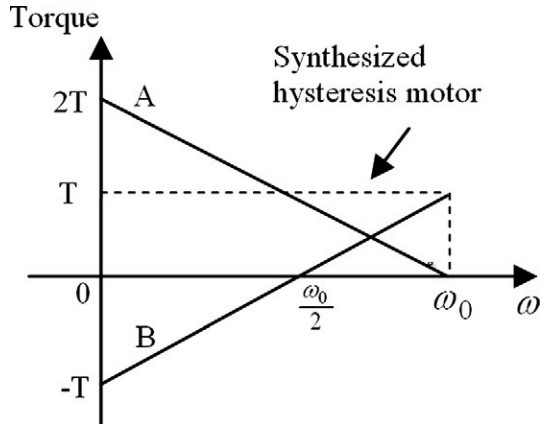

Fig. 12. The synthesized hysteresis motor.

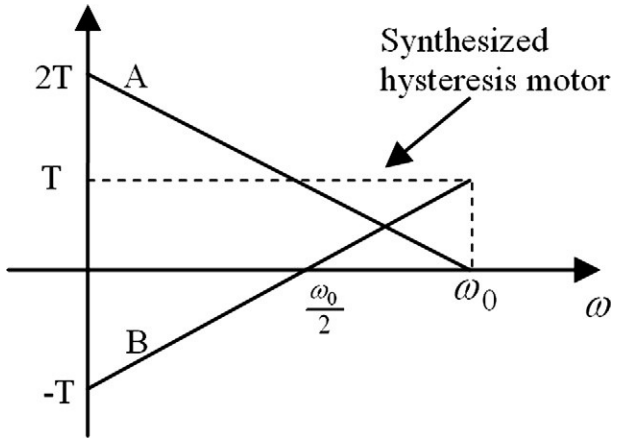

Fig. 13. Synthesized hysteresis motor from two induction motors.

winding whose resistance to reactance r_2/x_2 ratio is high as well will produce graph *B* as discussed earlier and shown in Fig. 12. The combination of the two linear graphs *A* and *B* produces a hysteresis motor torque–speed characteristics as shown in Fig. 12 as broken lines. At $\omega = 1/2\omega_0$, the torque of the TF machine is zero, graph B, the net torque of the hysteresis motor being provided by the SCIM.

At synchronous speed $\omega = \omega_0$, the torque of the SCIM is zero, the net torque being provided by the TF machine. The SCIM and the TF machine are arranged as shown in Fig. 10, their rotors being mechanically coupled together and their windings connected in parallel to the supply.

In view of the foregoing, it follows that a hysteresis motor can also be synthesized from two induction motors. Consider a two-pole squirrel cage induction motor (SCIM) with high rotor resistance to leakage reactance r_2/x_2 ratio coupled to a four-pole wound rotor induction motor (WRIM) and both connected to the same supply. Suppose the rotor winding of the latter is connected to a capacitive load through the slip rings in a manner akin to the connection of external rotor resistance to wound rotor induction motors. If the effective leakage reactance is capacitive, the power factor of the machine becomes leading, instead of the usually inductive lagging power factor. Consequently, the torque–speed characteristic of the machine will take the form of '*B*' as shown in Fig. 13, assuming high rotor r_2/x_2 ratio, and cutting the *x*-axis at $1/2\omega_0$, which is the synchronous speed of the four-pole induction motor, in comparison to the synchronous speed ω_0 of the two-pole SCIM. The four-pole induction motor will therefore operate in the generating mode in the low-speed region $0 \leqslant \omega \leqslant 1/2\omega_0$ and producing positive torque as a motor in the high speed range $1/2\omega_0 \leqslant \omega \leqslant \omega_0$. The result of the combination of the torque–speed characteristics of the two machines produces a hysteresis torque–speed characteristics as shown in Fig. 13.

7. Conclusion

The synthesis of a hysteresis motor from an induction motor with high rotor resistance to leakage reactance ratio and a TF machine which are mechanically coupled together and both connected in parallel to the supply has been presented. The synthesized hysteresis motor will not be as quiet in operation as the conventional hysteresis motor, but will exhibit the usual noise associated with conventional induction motors. By using a squirrel cage induction motor with high rotor r_2/x_2 ratio and a TF machine, the proposed hysteresis motor would be entirely brushless and consequently robust, requiring very little maintenance. In synthesizing a hysteresis motor from SCIM and WRIM, the stator magnetic poles of the WRIM for obvious reasons must be twice that of the SCIM so that its synchronous speed will be one-half that of the SCIM. In synthesizing from a SCIM and a TF machine, it requires that the two machines be wound for the same pole number since the TF machine is naturally a half-speed machine. Therefore, when both are wound for the same pole number, the synchronous speed of the TF machine is $1/2\omega_0$ while that of the SCIM is ω_0. The synthesis of a hysteresis motor although still in the analytical stage, it is expected that the output torque of the synthesized version can be made large and would drive as much load as the conventional induction motors. Consequently, the synthesized version will find applications in both domestic and industrial drives. The possibility of combining the TF machine and the induction motor comprising the hysteresis motor in a single frame is being vigorously pursued for improved convenience of use.

References

[1] Raham MA, Oseiba AM. Dynamic performance prediction of polyphase hysteresis motor. IEEE Trans Ind Appl 1990;26(6):1026–33.
[2] Awed Badeb OM. Investigation of the dynamic performance of hysteresis motors using Matlab/Simulink. J Electr Eng 2005;56(3–4):106–9.
[3] Kim HK, Jung HK, Hong SK. Finite element analysis of hysteresis motor using the vector magnetization-dependent method. IEEE Trans Magn 1998;34(5):3495–8.
[4] Agu LA. Synthesis of a motor with hysteresis motor type characteristics. In: Conference proc on new products and technologies for small and medium enterprises, University of Benin; 2001. p. 75–6.
[5] Gorges H. Veber Drestrommotoren mit verminderta Tourenzabl. Elektrotech Z 1896;17:517–8.
[6] Broadway ARW, Tan SCF. Brushless stator-controlled synchronous-induction machine. Proc IEE 1973;120(8):860–6.
[7] Agu LA. The transfer-field electric machine. Electric Mach Electromech 1978;2(4):403–18.
[8] Cathey JJ, Nasar SA. Equivalent circuit of transfer field machine for asynchronous mode of operation. Electric Mach Electromech 1981;6:307–21.
[9] Anih LU, Obe ES. Performance analysis of a composite dual winding reluctance machine. Energy Convers Manage 2009;50:3056–62.
[10] Anih LU. Magnetics of an idealized asynchronous reluctance machine with no moving conductors. Pac J Sci Technol 2009;10(1):82–92.
[11] Anih LU, Agu LA. Mechanism of torque production in a coupled polyphase reluctance machine. Nigeria J Technol (NIJOTECH) 2008;27(1):29–39.